JOURNAL OF PROPULSION AND POWER
Vol. 13, No. 1, January–February 1997

Optimal Control of Quasi-One-Dimensional Self-Field Magnetoplasmadynamic Arcjet Flowfields

Kyoichiro Toki*
Institute of Space and Astronautical Science, Sagamihara, Kanagawa 229, Japan

The flowfield of a self-field magnetoplasmadynamic (MPD) arcjet was analyzed to establish the optimum geometry that produces the highest possible thrust for specified operating conditions. A set of simplified assumptions, within a quasi-one-dimensional framework, was used to establish how the optimum flowfield was coupled to the thruster geometry. The resultant distribution of discharge current was smooth without any prominent concentration along the electrodes. The approach employed a purely mathematical method of engineering optimal control to suggest design guidelines for MPD arcjet thrusters within the idealized constraints. The optimum was found to be a slowly convergent and quickly divergent geometry that maximized the exit velocity for a fixed electrical input power.

Nomenclature

A = channel area, m^2 or nondimensional
A_0 = reference area, m^2 or nondimensional
B = magnetic flux density, weber/m^2 or nondimensional
B_0 = B at the inlet, weber/m^2 or nondimensional
E = electric field, V/m or nondimensional
J = total current, A
j = current density, A/m^2 or nondimensional
l = thruster length, m
$\dot{m}$ = mass flow rate, g/s
Rm = magnetic Reynolds number, nondimensional
u = plasma velocity, m/s or nondimensional
u_m = magnetic velocity, m/s
V = discharge voltage, V or nondimensional
w = thruster width, m
x = position along the channel, m or nondimensional
λ_1 = Lagrange multiplier, nondimensional
λ_2 = Lagrange multiplier, nondimensional
μ_0 = magnetic permeability, H/m
ρ = density, kg/m^3 or nondimensional
σ = electrical conductivity, /Ωm
$\sim$ = nondimensionalization

Subscript
i = inlet
e = exit

Introduction

THE self-field magnetoplasmadynamic (MPD) thruster is one of the promising electric propulsion technologies for future application to space missions.[1] For 30 years experimental and analytical studies have attempted to understand the physical processes controlling thruster operation to identify geometries that produce higher efficiency and select appropriate propellants.[2–4] Figure 1 exhibits stable geometric configurations from a variety of research organizations. Each organization has chosen a baseline thruster that reflects its primary area of interest, including pulsed or steady-state, self-field, or applied-field MPD arcjets.

In this report, a mathematical optimization is used to maximize performance independent of any experimental conclusions. While the model formulation is so idealized that most of the complicated physics associated with the actual plasma flow are ignored, this kind of optimization can provide useful guidance to MPD arcjet experimentalists. We have assumed the flowfield geometry to be quasi-one-dimensional to exclude all of the possible sources of ambiguity to the problem by virtue of their multidimensionality. A method of engineering optimal control, i.e., the calculus of variations, is applied. The ultimate purpose of this analysis is to unambiguously demonstrate the existence of an optimum quasi-one-dimensional MPD arcjet geometry that produces maximum thrust for a fixed discharge current, discharge voltage, mass flow rate, and thruster length.

Assumptions

For simplicity, we assume the following conditions: 1) particle pressure is ignored; 2) ionization and dissociation are ignored, and hence, σ has a constant value; 3) no external magnetic field; 4) quasi-one-dimensional flowfield, i.e., we ignore the pumping force, Hall effect, viscous boundary layer, and the electrical sheath; and 5) the onset phenomenon is ignored, although the high I_{sp} region is of interest.

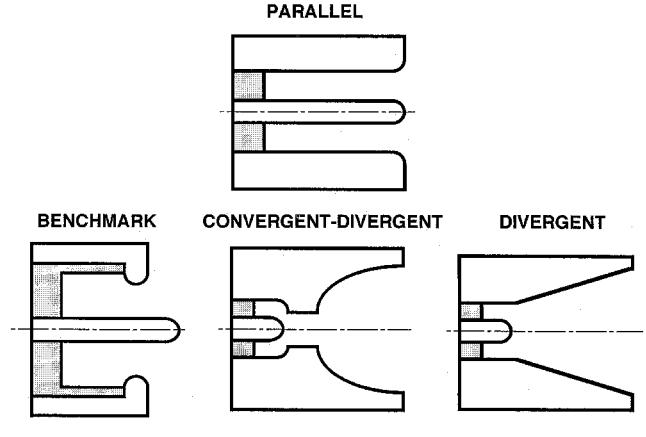

Fig. 1 Self-field MPD arcjet geometry variations.

Received Sept. 4, 1995; revision received May 1, 1996; accepted for publication Aug. 11, 1996.

*Associate Professor, Space Propulsion Division.

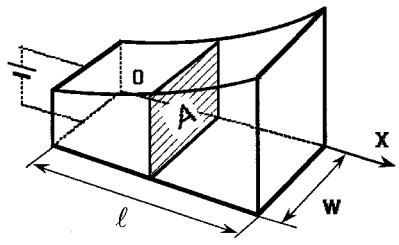

Fig. 2 Assumed quasi-one-dimensional MPD arcjet thruster channel.

For these assumptions we can define the geometry of our MPD arcjet thruster (Fig. 2). The equations are as follows:

Mass conservation:

$$\rho u A = \dot{m} \tag{1}$$

Momentum conservation:

$$\rho u \frac{\mathrm{d}u}{\mathrm{d}x} = j \cdot B \tag{2}$$

Maxwell's equation:

$$\frac{\mathrm{d}B}{\mathrm{d}x} = -\mu_0 j \tag{3}$$

Ohm's law:

$$j = \sigma(E - u \cdot B) \tag{4}$$

Equipotential condition:

$$AE/w = V \tag{5}$$

The last equation expresses the equipotential constraint over the entire electrode surface for the anode and cathode. We can reasonably exclude the energy conservation equation, because the particle pressure is ignored in this formulation. This assumes that the flow is only electromagnetically accelerated, and hence, Joule heating merely increases the temperature. The flow enthalpy does not contribute to the aerodynamic acceleration.

Fundamental Formulation

It is convenient to nondimensionalize the variables with some reference quantities describing the flow such as

Total current:

$$J = w \int_0^l j \, \mathrm{d}x = \frac{w}{\mu_0} B_0 \tag{6}$$

Magnetic velocity:

$$u_m = \frac{B_0^2 A_0}{\mu_0 \dot{m}} \tag{7}$$

Magnetic Reynolds number:

$$R_m = \mu_0 \sigma u_m l \tag{8}$$

Using these quantities, all of the variables are nondimensionalized:

$$\tilde{J} = \frac{J}{(w/\mu_0)B_0} \qquad \tilde{u} = u/u_m \qquad \tilde{\rho} = \rho u_m A_0/\dot{m} \tag{9}$$

$$\tilde{j} = (\mu_0 l/B_0)j \qquad \tilde{A} = A/A_0 \qquad \tilde{E} = E/u_m B_0 \tag{10}$$

$$\tilde{B} = B/B_0 \qquad \tilde{V} = Vw/A_0 u_m B_0 \qquad \tilde{x} = x/l \tag{11}$$

Hereafter, the nondimensionalized variables are used without a tilde mark, ~. Equations (1–5) are rewritten as

$$\rho u A = 1 \tag{12}$$

$$\rho u \frac{\mathrm{d}u}{\mathrm{d}x} = j \cdot B \tag{13}$$

$$\frac{\mathrm{d}B}{\mathrm{d}x} = -j \tag{14}$$

$$j = R_m(E - u \cdot B) \tag{15}$$

$$AE = V \tag{16}$$

We assign reasonable values to the following quantities: Rm = 10, J = 12.5 kA, l = 0.1 m, w = 0.1 m, A_0 = 0.001 m^2, and $\dot{m}$ = 1.25 g/s. These values correspond to u_m = 15.7 km/s and σ = 5071 /Ωm.

Numerical Experiment for Various Geometries

Prior to carrying out the optimization, the flowfield of the predetermined thruster geometry is analyzed for various cases. From Eqs. (12), (15), and (16), ρu, j, and E can be eliminated and substituted into Eqs. (13) and (14), respectively. Then we obtain a set of two equations to be solved:

$$\frac{\mathrm{d}u}{\mathrm{d}x} = R_m(V - AuB)B \tag{17}$$

$$\frac{\mathrm{d}B}{\mathrm{d}x} = -R_m(V - AuB)\frac{1}{A} \tag{18}$$

Initial conditions are required so that V satisfies the given value of R_m:

$$B(1) = 0 \tag{19}$$

In other words, this condition is required for Eq. (16), which implicitly corresponds to a differential equation ($\mathrm{d}V/\mathrm{d}x = 0$). The given total current must be equal to the integration of current density along the electrodes and the inlet velocity must be assumed:

$$B(0) = 1, \qquad u(0) = 0.5 \tag{20}$$

Figure 3 shows the calculated flowfields for Rm = 10 for parallel, convergent, divergent, and convergent–divergent thrusters. In this sample analysis, a parallel configuration with A = 4 was first calculated as the reference and the corresponding discharge voltage was obtained. A convergent, divergent, or convergent–divergent shape was then assumed in the form of $A = A(x) + c$, where c is a constant. The constant c was varied until a new geometry was found, yielding the same discharge voltage as the baseline, but having a different exit velocity. Thus, this procedure finds the highest performance geometry for a given input power. All of the calculations used the same discharge current, mass flow rate, thruster length, and discharge voltage. The different exit velocity yields a different thrust and efficiency for the given inputs. For all of these examples, the nondimensional discharge voltage is 4.70, which corresponds to an actual voltage of 116 V calculated from Eqs. (11). Each of the current distributions reveals strong concentration at the exit and the inlet of the thruster as a result of back emf in the middle region of the channel. The velocity distribution displays a slow acceleration region halfway to the exit. The plasma acceleration is far from constant in the streamwise direction.

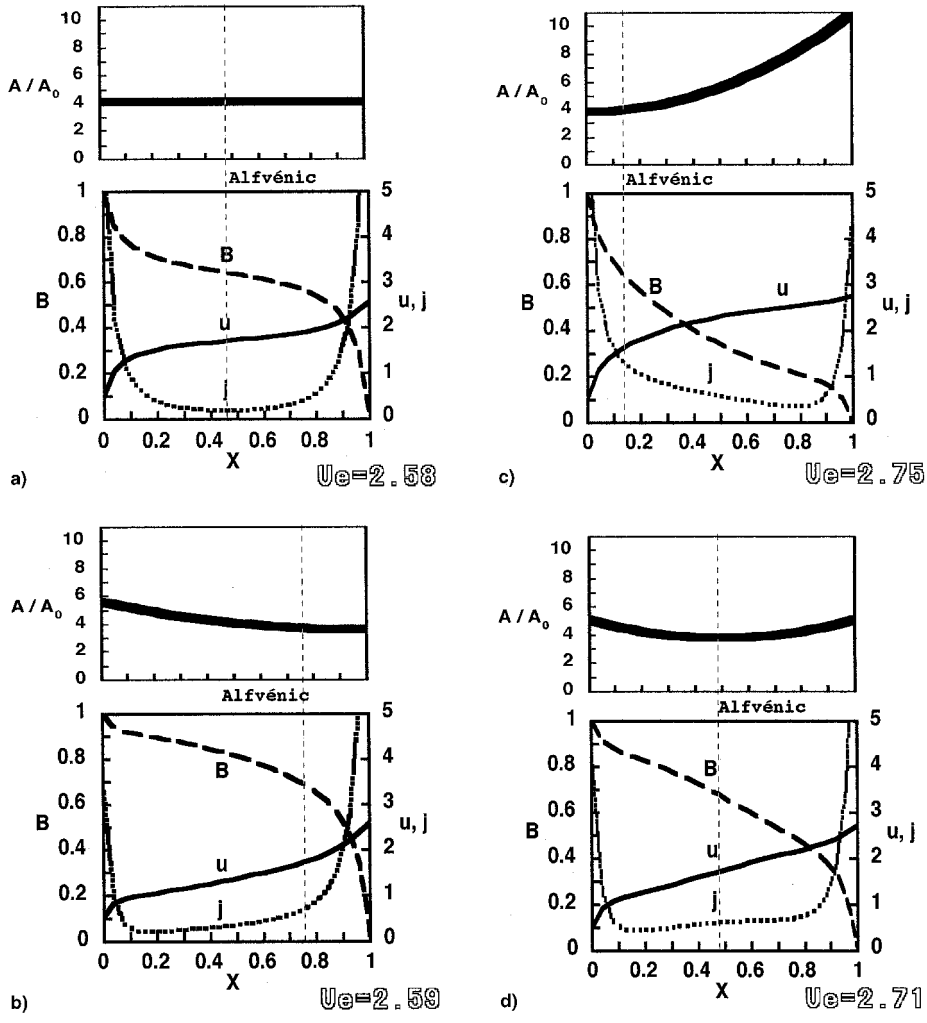

Fig. 3 Numerical experiment for various quasi-one-dimensional MPD arcjet geometries a) parallel, b) convergent, c) divergent, and d) convergent–divergent. All have the same discharge current and voltage with $Rm = 10$: each part shows specified geometry and flowfield analysis.

Method of Engineering Optimum Control

This section describes the mathematically optimum geometry. Here we introduce two new functions according to optimization theory,[5] the evaluation functional I, and the Lagrangian H

$$I = \int_0^1 \frac{du}{dx}\,dx = \int_0^1 R_m(V - AuB)B\,dx \tag{21}$$

$$H = (1 + \lambda_1)R_m(VB - AuB^2) + \lambda_2 R_m[uB - (V/A)] \tag{22}$$

where the optimum geometry maximizing the exit velocity must be found among the admissible geometry functions A. Two adjoint variables, λ_1 and λ_2, are incorporated because of the constraints represented by the differential equations (23) and (24), and finally, the Euler–Lagrange equations are obtained as follows:

$$\frac{du}{dx} = R_m(V - AuB)B \tag{23}$$

$$\frac{dB}{dx} = -R_m(V - AuB)\frac{1}{A} \tag{24}$$

$$\frac{d\lambda_1}{dx} = R_m\left[\frac{V - AuB}{Au}\right]\lambda_2 \tag{25}$$

$$\frac{d\lambda_2}{dx} = R_m\left[\frac{-(V - AuB)^2}{V}\right](1 + \lambda_1) \tag{26}$$

$$A^2 = \frac{V}{uB^2}\frac{\lambda_2}{1 + \lambda_1} \tag{27}$$

which, along with Eqs. (23) and (24), are the duplication of Eqs. (17) and (18). If there exists an optimum geometry having the maximum exit velocity, it is required to be the solution of these differential equations.

The previous simultaneous differential equations define a two-point boundary-value problem, therefore, some of the initial (inlet) and final (exit) conditions must be given. Table 1 summarizes the boundary conditions, including a transversality condition for the adjoint variables. We applied the direct shooting method (DSM) to solve this two-point boundary-value problem, where the values of $\lambda_1(0)$ and $\lambda_2(0)$ are initially assumed and sequentially modified by linearized approximation of the residual error until $B(1) = 0$ and $\lambda_1(1) = 0$ are simultaneously satisfied.

Optimum Geometry

Solving Eqs. (23–27) under the same J, V, $\dot{m}$, and λ values as adopted in the preceding numerical experiment, the optimum geometry for $Rm = 10$ was calculated and presented in Fig. 4. The maximum calculated nondimensional exit velocity is 2.88 as shown in Table 2, resulting in an efficiency improve-

Table 1 Boundary conditions

Initial	Final
$u(0) = 0.5$	——
$B(0) = 1$	$B(1) = 0$
——	$\lambda_1(1) = 0$

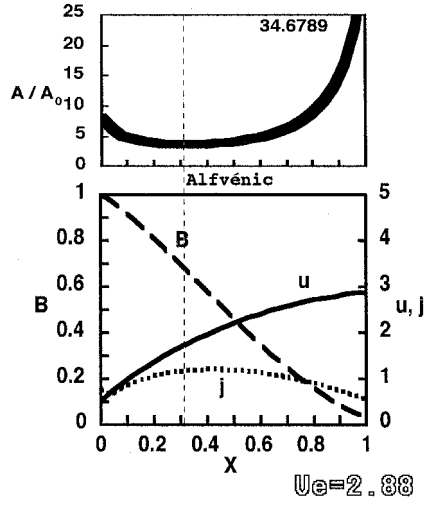

Fig. 4 Optimum geometry for $Rm = 10$ (top, obtained geometry and bottom, obtained flowfield).

ment of 25% over the baseline geometry for the given input power. The geometry is slowly convergent at the rear, followed by a highly divergent channel for high magnetic Reynolds number. The most remarkable feature of this flowfield is the moderately uniform current distribution over the entire channel. This contrasts with the other geometries that exhibit strong current concentration at both the inlet and the exit (see Fig. 3).

The more uniform current distribution results in a velocity distribution with a steady acceleration pattern, free from any deflection-like nonuniformities that would result from strong current concentrations. A similar suggestion for this kind of geometry has been made previously.[6] The optimum geometry requires a very steep divergence angle at the exit and it seems to be outside the scope of quasi-one-dimensionality. A similar optimization procedure was used at very low Rm less than unity, although the assumption $Rm < 1$ is not valid for MPD thrusters. That effort showed that a convergent geometrical shape was optimum for $Rm < 1$.

Discussion

General Understandings of Results

The optimum geometry was calculated for $Rm = 10$. It is interesting that there may be an analogy between the magnetized plasma flow (magnetic pressure dominant) and the aerodynamic flow (particle pressure dominant) of a De Laval nozzle. This parallel has been reported previously to emphasize the importance of magnetic Reynolds number in the MPD flowfield,[6–8] and precise calculations were performed for various predetermined but nonoptimized geometries.[8] Furthermore, recent experiments using a two-dimensional MPD arcjet have shown that the best performance is achieved in the case of a convergent–divergent channel.[9]

Apparently, the optimum geometry yields continuous acceleration throughout the MPD channel. The abrupt velocity increases observed at the inlet and exit of nonoptimum geometries have completely disappeared. For high Rm values, it has been reported that the discharge voltage is determined by the deflection point of the magnetic pressure profile along the channel.[10] The strong current concentration at the edges of a channel always enhances Joule heating effects, leading to the loss of input power. This has been regarded as an unavoidable feature in so far as the Rm remains finite in the actual MPD flowfield.

Table 2 Comparison of arbitrary geometry and the optimum

Geometry	Exit velocity, u_e, nondimensional	Improvement over parallel efficiency, %
Parallel	2.58	0
Convergent	2.59	0.7
Convergent–divergent	2.71	10
Divergent	2.75	14
Optimum	2.88	25

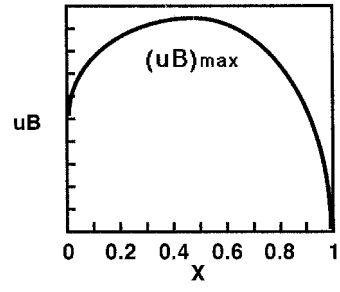

Fig. 5 Representative uB profile at high Rm values.

Physical Interpretation

Substituting Eq. (14) into Eq. (13) and multiplying by u, we obtain an interesting relationship after a simple transformation of the equation:

$$\left(\frac{B^2}{\rho} - u^2\right)\frac{du}{dx} = \frac{B}{\rho}\frac{d}{dx}(uB) \tag{28}$$

If u reaches $u^2 = B^2/\rho$ (the Alfvén speed or, exactly speaking, the magnetosonic speed), then $d/dx(uB) = 0$ should be satisfied. From the boundary conditions for inlet and exit of the channel

$$(uB)_{\text{exit}} = 0 \qquad (uB)_{\text{inlet}} = u_i < 1 \tag{29}$$

Provided that the acceleration is monotonic along the streamwise direction, the following point will be met somewhere along the channel (Fig. 5):

$$uB = (uB)_{\max} \tag{30}$$

On the other hand, from Ohm's law, Eq. (15):

$$V/A = uB + (j/R_m) \tag{31}$$

If there is some point where $j >> 1$, V is mainly determined by the value of j/Rm at that point. Multiplying Eq. (31) by jA

$$jV = uBjA + (j^2/R_m)A \tag{32}$$

where the left-hand side is the local input power, and the first term of the right-hand side corresponds to the local acceleration power (Lorentz power) for the flow. Using Eqs. (12) and (13), the first term is transformed to

$$uBjA = u \cdot \rho u \frac{du}{dx} \cdot A = \frac{1}{2}\frac{du^2}{dx} \tag{33}$$

The integration over the entire channel for this term represents the total thrusting power, and the second term in Eq. (32) is the overall Joule heating power. From this derivation, at the point where $j >> 1$, Joule heating exceeds the Lorentz power. Therefore, the input power cannot contribute to effective ac-

celeration of the flow. By contrast, provided that $j << Rm$ is satisfied over the entire channel, except for where B is zero (the exit), Eq. (32) can be expressed as

$$V/A = uB + \mathcal{O}(R_m^{-1}) \tag{34}$$

Here, the discharge voltage is mainly determined by uB, the so-called back-emf. Once V is determined, its value is constant over the channel and the geometry A is determined by the inverse of uB values. A typical uB profile is presented in Fig. 5. This consequently requires the convergent–divergent shape, eliminating the extreme current concentration.

In the optimum solution, the discharge voltage is determined by uB under the condition of high Rm values, or $j << Rm$. In the nonoptimum solution, because of strong current concentration at the inlet and the exit, whichever term is dominant, (j/R_m or uB), determines the discharge voltage. Note that the actual MPD flowfield has three-dimensional characteristics relaxing the current concentration at the exit of the channel by forming a virtual cathode with axial current inflow. Also, the real-gas effect of ionization/dissociation suppresses the inlet current concentration. Although these smoothing effects appearing in the actual current distribution may compensate for the disadvantage of nonoptimum geometry, they do not imply a major improvement on the thruster performance. The optimization here has essentially eliminated the severe current concentration and has logically achieved a thrust performance improvement.

Conclusions

An optimum geometry producing the highest thrust performance for a given input power was calculated under the framework of an idealized quasi-one-dimensional self-field MPD flowfield. The optimum geometry was established for high Rm (=10) and specified discharge current, discharge voltage, and mass flow rate. The optimum geometry, corresponding to that yielding the highest exhaust velocity for a given voltage, was found to be a slowly convergent shape in the upstream region with a quickly divergent shape in the downstream region. This optimum geometry results in a uniform current distribution compared to nonoptimized geometries, and yields a 25% efficiency improvement over a simple parallel electrode geometry.

Acknowledgment

The author extends his thanks to Kyoichi Kuriki for many fruitful discussions on this problem.

References

[1]Toki, K., Shimizu, Y., Kuriki, K., and Kuninaka, H., "An MPD Arcjet Thruster System for Electric Propulsion Experiment (EPEX) in Space," AIAA Paper 94-2989, June 1994.

[2]Wegmann, T., Auweter-Kurtz, M., Habiger, H., and Schrade, H., "Experimental Comparison of Steady State Nozzle Type and Cylindrical MPD Thrusters at High Current Levels," International Electric Propulsion Conf., Paper 93-122, Sept. 1993.

[3]Sovey, J. S., and Mantenieks, M. A., "Performance and Lifetime Assessment of Magnetoplasmadynamic Thruster Technology," *Journal of Propulsion and Power*, Vol. 7, No. 1, 1991, pp. 71–83.

[4]Hoskins, W. A., Kelly, A. J., and Jahn, R. G., "Asymmetric Discharge Patterns in the MPD Thruster," AIAA Paper 90-2666, July 1990.

[5]Wu, K. A., and Miele, A., "Sequential Conjugate Gradient-Restoration Algorithm for Optimal Control Problems with Non-Differential Constraints and General Boundary Conditions, PART-1, PART-2," *Optimal Control Applications and Methods*, Vol. 1, No. 1, 1980, pp. 69–80.

[6]Heimerdinger, D. J., and Martinez-Sanchez, M., "Effect of Axial Variation of Electrode Spacing on MPD Arcjet Behavior," AIAA Paper 87-0998, 1987.

[7]Kuriki, K., Kunii, Y., and Shimizu, Y., "Idealized Model for Plasma Acceleration in an MHD Channel Flow," *AIAA Journal*, Vol. 21, No. 3, 1984, pp. 322–326.

[8]Martinez-Sanchez, M., "Structure of Self-Field Accelerated Plasma Flow," *Journal of Propulsion and Power*, Vol. 7, No. 1, 1991, pp. 56–64.

[9]Funakai, I., Toki, K., and Kuriki, K., "Role of Anode Throat in MPD Arcjet," International Electric Propulsion Conf., Paper 93-120, Sept. 1993.

[10]Kuriki, K., and Nakayama, T., "Magnetosonic Condition in Magnetoplasmadynamic Flow," *Journal of Propulsion and Power*, Vol. 8, No. 6, 1992, pp. 1208–1211.